



AMERICAN METEOROLOGICAL SOCIETY

Bulletin of the American Meteorological Society

EARLY ONLINE RELEASE

This is a preliminary PDF of the author-produced manuscript that has been peer-reviewed and accepted for publication. Since it is being posted so soon after acceptance, it has not yet been copyedited, formatted, or processed by AMS Publications. This preliminary version of the manuscript may be downloaded, distributed, and cited, but please be aware that there will be visual differences and possibly some content differences between this version and the final published version.

The DOI for this manuscript is doi: 10.1175/BAMS-D-18-0057.1

The final published version of this manuscript will replace the preliminary version at the above DOI once it is available.

If you would like to cite this EOR in a separate work, please use the following full citation:

Santoso, A., H. Hendon, A. Watkins, S. Power, D. Dommenges, M. England, L. Frankcombe, N. Holbrook, R. Holmes, P. Hope, E. Lim, J. Luo, S. McGregor, S. Neske, H. Nguyen, A. Pepler, H. Rashid, A. Sen Gupta, A. S. Taschetto, G. Wang, E. Abellán, A. Sullivan, M. Huguenin, F. Gamble, and F. Delage, 2018: Dynamics and predictability of the El Niño-Southern Oscillation: An Australian perspective on progress and challenges. *Bull. Amer. Meteor. Soc.* doi:10.1175/BAMS-D-18-0057.1, in press.



Dynamics and predictability of the El Niño-Southern Oscillation: An Australian perspective on progress and challenges

Agus Santoso^{1,2,3}, Harry Hendon⁴, Andrew Watkins⁴, Scott Power⁴, Dietmar Dommenges^{5,6},
Matthew England^{1,2}, Leela Frankcombe^{1,2}, Neil Holbrook^{7,8}, Ryan Holmes^{1,2,9}, Pandora
Hope⁴, Eun-Pa Lim⁴, Jing-Jia Luo^{4,10}, Shayne McGregor^{5,6}, Sonja Neske^{5,6}, Hanh Nguyen⁴,
Acacia Pepler⁴, Harun Rashid¹¹, Alex Sen Gupta^{1,2}, Andréa S. Taschetto^{1,2}, Guomin Wang⁴,
Esteban Abellán¹, Arnold Sullivan¹¹, Maurice Huguenin¹², Felicity Gamble⁴, Francois
Delage⁴

¹*Climate Change Research Centre and ARC Centre of Excellence for Climate System Science,
University of New South Wales, Sydney, Australia*

²*ARC Centre of Excellence for Climate Extremes, University of New South Wales, Sydney, Australia*

³*Centre for Southern Hemisphere Oceans Research, CSIRO Oceans and Atmosphere, Hobart,
Australia*

⁴*Australian Bureau of Meteorology, Melbourne, Australia*

⁵*School of Earth, Atmosphere, and Environment, and ARC Centre of Excellence for Climate System
Science, Monash University, Melbourne, Australia*

⁶*ARC Centre of Excellence for Climate Extremes, Monash University, Melbourne, Australia*

⁷*Institute for Marine and Antarctic Studies, University of Tasmania, Hobart, Australia*

⁸*ARC Centre of Excellence for Climate Extremes, University of Tasmania, Hobart, Australia*

⁹*School of Mathematics and Statistics, University of New South Wales, Sydney, Australia*

¹⁰*Collaborative Innovation Center on Forecast and Evaluation of Meteorological Disasters /KLME /
ILCEC, Nanjing University of Information Science and Technology, Nanjing, China*

¹¹*CSIRO Oceans and Atmosphere, Aspendale, Australia*

¹²*Institute for Atmospheric and Climate Science, ETH Zürich, Zürich, Switzerland*

Corresponding author: Agus Santoso (a.santoso@unsw.edu.au)

For *Bulletin of the American Meteorological Society* (Essay)

Capsule summary (30 words max.): Many scientific challenges remain that need to be addressed in order to manage risk of future ENSO impacts in countries like Australia that are strongly affected by ENSO event diversity.

Abstract:

El Niño and La Niña, the warm and cold phases of the El Niño Southern Oscillation (ENSO), cause significant year-to-year disruptions in global climate including in the atmosphere, oceans and cryosphere. Australia is one of the countries where its climate, including droughts and flooding rains, is highly sensitive to the temporal and spatial variations of ENSO. The dramatic impacts of ENSO on the environment, society, health, and economies worldwide make the application of reliable ENSO predictions a powerful way to manage risks and resources. An improved understanding of ENSO dynamics in a changing climate has the potential to lead to more accurate and reliable ENSO predictions by facilitating improved forecast systems. This motivated an Australian national workshop on ENSO dynamics and prediction that was held in Sydney, Australia, in November 2017. This workshop followed the aftermath of the 2015/16 extreme El Niño which exhibited different characteristics to previous extreme El Niños and whose early evolution since 2014 was challenging to predict. This essay summarizes the collective workshop perspective on recent progress and challenges in understanding ENSO dynamics and predictability, and improving forecast systems. While this essay discusses key issues from an Australian perspective, many of the same issues are important for other ENSO-affected countries, and for the international ENSO research community.

1. Motivation

1.1. The Australian context

ENSO has long been recognized to strongly influence global and regional climate. Australian climate is particularly impacted by ENSO (e.g., McBride and Nicholls 1983; Ropelewski and Halpert 1987; Power et al. 1998). The associated changes in circulation, rainfall and temperatures are strong enough to impact its terrestrial and marine ecosystems (e.g. Nicholls 1985, 1991; Norman and Nicholls 1991; Holbrook et al. 2009). Although the impact can vary markedly from decade to decade (Power et al. 1999), bushfires, heatwaves and droughts generally tend to be more severe during El Niño years (e.g., Williams and Karoly 1999; Loughran et al. 2016), while the frequency of tropical cyclones across the north and flooding throughout much of the east tend to be enhanced during La Niña (e.g., Nicholls 1979; Werner and Holbrook 2011; Power and Callaghan 2016). To provide timely information on the likelihood of upcoming disruption of climate, ENSO outlooks have been issued routinely by the Australian Bureau of Meteorology since 2000.

The complex dynamics of ENSO manifest in diverse spatial and temporal evolution across events that lead to differing regional impacts (e.g., Power et al. 1999; Ashok et al. 2007; Wang and Hendon 2007; Capotondi et al. 2015a). For instance, in Australia, the magnitude of an El Niño event alone does not provide clear guidance on its impacts (Power et al. 2006; Wang and Hendon 2007; Chung and Power 2017). For example, the impact of the 1997/98 extreme El Niño was limited to the south-eastern region and Tasmania, but much more severe and widespread drought occurred during the moderate 2002/03 El Niño (Wang and Hendon 2007; Taschetto and England 2009; Lim and Hendon 2015), leading to a massive 25% drop in agricultural output (Lu and Hedley 2004).

The 2002/03 event was not only notably weaker in intensity than the 1997/98 extreme event, but also exhibited a characteristically different pattern of sea surface temperature (SST) anomalies. The 1997/98 El Niño had SST anomalies ($\sim +3^{\circ}\text{C}$) that peaked toward South America while those during 2002/03 event peaked in the central Pacific ($\sim +1^{\circ}\text{C}$). The contrast in spatial patterns fits the notion of two archetype structures of ENSO: “Eastern Pacific” (EP) and “Central Pacific” (CP) events (e.g., Ashok et al. 2007; Kao and Yu 2009) following an earlier assessment of ENSO SST patterns by Trenberth and Stepaniak (2001). This is illustrated in Fig. 1 which also shows that an event may not necessarily fall into either category – a pattern that is a mix of EP and CP types is possible as part of the ENSO continuum arising from non-linear dynamics, stochasticity, and remote forcing, which can also give rise to temporal evolution diversity (e.g., Takahashi et al. 2011; Dommenget et al. 2013; Lee et al. 2014; Takahashi and Dewitte 2016). This intrinsic ENSO complexity was recently summarized by Timmermann et al. (2018). As such, a clear classification of certain ENSO events into EP and CP can be difficult and be sensitive to the choice of index (e.g., Capotondi et al. 2015a).

The typical surface temperature and rainfall anomaly patterns associated with EP and CP ENSO are different over Australia, as well as other regions across the globe (Fig. 2). Specifically, CP events tend to be associated with larger and more widespread rainfall and temperature changes in Australia than EP events – analogous to the difference in impacts between the 2002/03 and 1997/98 events, even though EP El Niños tend to be stronger than CP events (e.g., Capotondi et al. 2015a; Fig. 1). Investigating the cause for the differing impact between EP and CP events is still an open area of research, but based on investigating the difference between 2002/03 and 1997/98 events, the contrast may be due to the forcing center of CP events that is closer to Australia (Wang and Hendon 2007; Lim and Hendon 2015). This could also illustrate the more general result, that impacts in Australia are more

tightly linked to the magnitude of La Niña than they are to the magnitude of El Niño (Power et al. 2006), as stronger La Niña events tend to be of a CP type (Fig. 1). As such, predicting the spatial structure of ENSO events is important for impact preparedness over regions like Australia (Hendon et al. 2009). Apart from classification of individual events, other factors such as event precursors, local processes (e.g., antecedent soil moisture, anomalies in regional seas), random disturbances, as well as other modes of climate variability, also matter in determining impacts.

The Australian continent extends from the tropics to the mid-latitudes, and is surrounded by warm tropical Indo-Pacific oceans to the north and the Southern Ocean to the south. Thus, it is not only affected by direct tropical impacts of ENSO via the Southern Oscillation but also by extratropical teleconnections due to ENSO-induced changes in tropical convection.

Furthermore, Australian climate is affected by a rich interplay between ENSO and other climatic events such as the Indian Ocean Dipole (IOD) and the Southern Annular Mode (SAM) (e.g. Hendon et al. 2007; Meyers et al. 2007; Risbey et al. 2009; Cai et al. 2011; Taschetto et al. 2011; Pui et al. 2012; Lim and Hendon 2015). Ocean surface temperature variations surrounding northern Australia, which tend to covary with ENSO also exert strong influence on Australian climate (e.g., Drosowsky and Chambers 2001; Hendon et al. 2012; Ummenhofer et al. 2015) and may even affect development of ENSO itself (Nicholls 1984).

This complexity of impacts and interactions combined with the uniqueness of every ENSO event poses grand challenges for predicting Australian climate. For example, unlike the extreme 1997/98 event, the extreme 1982/83 El Niño, which is also classified as an EP event, had a particularly strong impact on Australia, likely due to relatively strong cold sea surface anomaly to the north-northeast of Australia (van Rensch et al. 2015). Severe drought gripped the eastern half of the country, marked by the historically catastrophic ‘Ash Wednesday’

bushfires in the southeast (Voice and Gauntlett 1984). For these reasons, and given Australia's susceptibility to future climate change, ENSO is at the forefront of climate research in Australia.

1.2. Unexpected turns of events

Following the extreme El Niño events in 1982/83 and 1997/98, the most recent major El Niño event occurred in 2015/16 (Blunden and Arndt 2016; Xue and Kumar 2017; L'Heureux et al. 2017). This first extreme El Niño of the 21st Century (Santoso et al. 2017) followed a “false alarm” in 2014. In 2014, the equatorial Pacific warm water volume (WWV) increased rapidly during the austral autumn following a strong westerly wind burst (WWB) event, reaching a level not seen since 1997 (McPhaden 2015). Increased WWV and increased activity of WWBs are typical precursors for an El Niño (see Table 1 for WWV and WWB definitions). However, the much anticipated big El Niño did not emerge at the end of 2014 (Hannam 2014), but it did instead in 2015.

The “roller-coaster” evolution of the 2014-2016 events and their prediction are illustrated in Figure 3, using the *ENSO Outlook* indicator from the Australian Bureau of Meteorology. The Bureau raised its *ENSO Outlook* to “watch” in February and March 2014, and subsequently elevated to “alert” in April-July, indicating the increasing possibility of an El Niño (of any magnitude) later in the year. This coincided with a spike in WWV that often precedes El Niño events, in line with the ENSO recharge oscillator theory (Jin 1997). However, the outlook status was downgraded back to “watch” in August-October, and then elevated again to “alert” in November-January. This outlook variation appears to be in line with WWV decline since the previous April before a slight increase again around July. A strong El Niño never materialized, which was later shown to be due to a combination of impeding factors, such as muted WWB activity (Menkes et al. 2014) and an occurrence of intense easterly wind

burst (Hu and Fedorov 2016), as well as a mean-state associated with the negative phase of the Interdecadal Pacific Oscillation (IPO) that is less favourable for Bjerknes feedbacks at the root of El Niño growth (Wang and Hendon 2017) and an anomalously warm Indian Ocean surface (Dong and McPhaden 2018) – both factors are associated with stronger Pacific Walker Circulation. The tropical Pacific was nonetheless left anomalously warm, but fell short to being considered an El Niño condition (e.g., Santoso et al. 2017).

In early 2015 clear signs of an emerging El Niño were detected, and the outlook status was raised to “event” in May 2015 (Watkins 2015). A strong El Niño developed in the latter half of 2015. The tropical Pacific then cooled, with a borderline La Niña developing in austral summer of 2016-17 declared by some agencies (but not the Bureau) followed by the Bureau’s official declaration of a weak La Niña in December 2017.

Amidst the widespread speculation in early 2014 of a strong El Niño that year, the Bureau’s coupled model, POAMA (Predictive Ocean Atmosphere Model for Australia), predicted only a weak event when initialized in austral autumn 2014 (Wang and Hendon 2017; see their Fig. 3a). In contrast, other models surveyed by the Bureau predicted a strong El Niño for 2014 (<http://www.bom.gov.au/climate/ahead/archive/models/201405-ms.shtml>). On the other hand, while issuing a stronger forecast for El Niño in 2015 than in 2014, POAMA initially underestimated the strength of the 2015/16 El Niño (Fig. 3b of Wang and Hendon 2017; the observed Niño3 falls outside the forecast 5-95% uncertainty range), and was weaker than the other surveyed models, until POAMA was initialized with late austral winter conditions (see the Bureau’s 2015 archive; e.g., <http://www.bom.gov.au/climate/ahead/archive/models/201508-ms.shtml>). This is not surprising though as predicting the magnitude of ENSO is challenging, more so than predicting the phase, especially early in the year when signal-to-noise ratio is low.

The challenge in anticipating and predicting the evolution and magnitude of the 2014-2016 chain of events, led to much retrospection about the state of our understanding of ENSO dynamics beyond the classical recharge-discharge oscillator theory, as well as the current state of the art climate models used to make predictions.

At an international ENSO workshop held in Sydney in 2015, key aspects of ENSO extremes and the associated open questions were discussed (Santoso et al. 2015). However, at that meeting, our knowledge of extreme El Niño was largely based on the 1982/83 and 1997/98 events – the only two extreme El Niño events in the modern instrumental record that showed distinct characteristics from other ENSO events. These characteristics include: (i) intense WWB activity in the western/central Pacific during event onset and development phases; (ii) a dramatic eastward and equatorward shift of atmospheric convection as El Niño emerges and matures, thereby inducing unusually high rainfall in the climatologically dry and cold eastern equatorial Pacific; and (iii) prominent eastward propagation of anomalous SSTs along the equatorial Pacific Ocean over event onset to decay phase¹. However, the latter two properties, which had previously been thought to typify an extreme El Niño, were less apparent during the 2015/16 El Niño (Santoso et al. 2017). In particular, while the 2015/16 El Niño did produce heavy rainfall over the eastern equatorial Pacific with December-February average rainfall in the Niño3 region (5°S-5°N, 150°W-90°W) close to 5 mm day⁻¹, a threshold used by Cai et al. (2014) to define an extreme El Niño, it exhibited record breaking rainfall over the Central Pacific, in stark contrast to the relatively weak El Niño-related rainfall in 1982/83 and 1997/98 events (Santoso et al. 2017).

¹ The propagation signature is diagnosed as the time-longitude slope of maximum equatorial SST anomaly (5°N-5°S average) over 160°E – 80°W from May of the El Niño development year to the following May when the event subsides, following Santoso et al. (2013).

The peculiarity of the 2015/16 event, the volatile 2014-2015 ENSO outlook (Fig. 3) and the complex ENSO behaviour and its impacts over Australia (section 1.1), motivated a second workshop on ENSO dynamics and prediction which was held in Sydney, Australia in November 2017 and involved 25 Australian ENSO researchers (www.climate-science.org.au/content/1182-enso-dynamics-workshop). Here we present the outcomes of this workshop, outlining recent research progress, knowledge gaps, impediments and recommendations to further advance ENSO research and prediction systems and service. These issues are discussed within each of five themes outlined in section 2, based largely on the studies presented by the workshop participants as referenced therein. A summary is provided in section 3 along with closing remarks on infrastructures and synergy behind ENSO research in Australia. Definitions of some terminologies discussed in the paper are provided in Table 1.

2. Discussions

2.1. Insights from the 2015/16 El Niño

The emergence of the strong 2015/16 El Niño showed that an extreme El Niño does not necessarily exhibit SST anomalies peaking toward the far eastern Pacific as in the 1982/83 and 1997/98 events, which have until recently been used as a benchmark for defining an extreme El Niño (see Santoso et al. 2017 for a review). The global climate context for the 2015/16 El Niño was different from that for the 1982/83 and 1997/98 events (see also Newman et al. 2018). For instance, there was a much more significant and persistent signature of extra-tropical influence in the 2015/16 El Niño, with warm SST anomalies extending from the north-eastern Pacific to the Central Pacific associated with the North

218 Pacific Meridional Mode, than in the 1982/83 and 1997/98 events (Santoso et al. 2017; Paek
219 et al. 2017).

220 Unlike the previous two extremes, the large amplitude of the 2015/16 El Niño was built upon
221 an already abnormally warm tropical Pacific from 2014, rather than relying solely on a
222 vigorous Bjerknes feedback (Abellán et al. 2017). The weak 2014/15 El Niño-like condition
223 prevented a large discharge of warm water out of the equatorial Pacific (Levine and
224 McPhaden 2016) that would normally occur following a strong El Niño. This allowed
225 anomalous equatorial warming to persist into 2015, priming the ocean for the subsequent El
226 Niño. The suite of processes leading up to the 2015/16 El Niño, along with a build-up of
227 ocean heat content in the off-equatorial Western Pacific over the previous decade, may have
228 triggered a shift in the phase of the IPO, from negative before to positive after 2014 (Meehl et
229 al. 2016). This can be invoked to partially explain the difference in amplitude between the
230 2014/15 and 2015/16 events (Wang and Hendon 2017), as a mean state associated with a
231 positive IPO is more conducive to the Bjerknes positive feedbacks for El Niño development
232 in the eastern Pacific (e.g., Zhao et al. 2016) – although the IPO itself is, in turn, partially a
233 long-term imprint of ENSO variability (Power and Colman 2006; Newman et al. 2016). The
234 subsequent decay of the 2015/16 event was also different from the 1982/83 and 1997/98
235 events in that it had persistent warm SST anomalies near the dateline, which lingered right
236 through the austral fall of 2016 and significantly delayed the Bjerknes feedback required for
237 the development of a following La Niña (Lim and Hendon 2017).

238 The distinctive characteristics of the 2015/16 extreme El Niño demonstrate that our
239 observational record is still too short to fully sample the diversity of ENSO characteristics.
240 Furthermore, there are uncertainties in observed SST data prior to the satellite era especially
241 before the 1950s when observations were sparse and ship recording practices were not

homogeneous (e.g., Ishii et al. 2005). This is particularly the case for meteorological variables over the ocean, meaning that comparisons to past events using a single index based on SST, and other variables for that matter, may not be accurate in terms of relative strength or variability. These issues mean that multiple observational products and indices beyond the commonly used ENSO metrics in operational forecast (e.g., Niño3.4, WWV, WWB, Southern Oscillation Index) are required to capture the diversity of ENSO extremes. Refinement of existing indices is also needed to better describe ENSO event diversity (e.g., Sullivan et al. 2016). In addition, the background climate upon which ENSO evolves is changing due to greenhouse warming and internal multi-decadal variability. To detect these long-term changes and the impact on ENSO characteristics, continuous high-quality observations are critical and so are reliable paleo-reconstructions for resolving characteristics of past ENSO events.

2.2. ENSO predictability

According to conventional ENSO theory (e.g., Jin 1997), WWV is a key precursor and hence predictor for ENSO. Consequently, WWV or the associated subsurface information is utilized in initializing forecast models to help alleviate the drop in ENSO prediction skill in austral autumn – widely known as the “(boreal) spring predictability barrier” (Webster and Yang 1992). However, anomalous WWV, while necessary, is not the only requirement for development of ENSO events, as demonstrated by the 2014 case. El Niño is typically triggered by a series of WWBs in the western/central Pacific (Vecchi and Harrison 2000). On the other hand, a negative WWV anomaly during austral autumn appears to be a better predictor for strong La Niña events than any other type of ENSO event (Santoso et al. 2017).

265 A better understanding of the relationship between WWV, WWB, and ENSO is important in
266 ENSO prediction.

267 On this front, Neske and McGregor (2018) showed that WWBs themselves can create a
268 significant WWV response that can be decomposed into two components: the “adjusted
269 response” (which relies on slow ocean dynamics associated with Rossby wave reflection as
270 depicted by the recharge oscillator theory) and the “instantaneous response” (which
271 represents surface Ekman transport in response to WWB). The adjusted response is identified
272 as the source of predictability and it has weakened since the start of the 21st Century – the
273 reason for this decline remains unclear but may be associated with a shift in the background
274 climate toward the cold phase of the IPO (Zhao et al. 2016) through modulation of governing
275 ENSO processes (e.g., WWBs, WWV, etc.). The instantaneous response, which has increased
276 in prominence in recent decades, emphasizes that ENSO is event-like rather than cyclical.
277 This research highlights that the balance of the two components can vary on decadal time
278 scales, giving rise to decadal modulation of ENSO predictability.

279 ENSO predictability does not lie solely within the tropical Pacific. Climate variability in
280 other oceanic basins also plays a role. Remote climate anomalies induce atmospheric
281 changes that are transmitted into the tropical Pacific through atmospheric planetary waves or
282 changes in the Walker Circulation, thereby affecting ENSO evolution. This remote influence
283 is highlighted by two recent studies that investigated the predictability of recent La Niña
284 events. Using two coupled models, Luo et al. (2017) showed that the Indian and Atlantic
285 Ocean warming contributed to the two-year lead predictability of the 2010-2012 series of La
286 Niña events. The multi-year surface warming in these oceans enhanced the Trade Winds over
287 the central-western Pacific that tend to favour La Niña development. The role of the Indian
288 Ocean was emphasized by Lim and Hendon (2017) who showed that the appearance of La

Niña in 2016, although weak, was promoted by earlier than normal development of a record strong negative IOD, which tends to enhance convection over the Indo-Pacific warm pool thereby strengthening the Pacific Trade Winds. They showed that using realistic ocean conditions in the Indian Ocean in late April 2016 was sufficient to produce the strong negative IOD during austral winter and spring and was necessary for delivering an improved La Niña forecast.

2.3. Response to greenhouse forcing

While the Pacific Ocean is projected to warm in the future, and that the anthropogenic warming is already evident in the western part of the basin (Wang et al. 2016), there is still uncertainty around whether ENSO events (typically measured through equatorial Pacific SST anomalies) will change in terms of their spatial patterns, amplitude, and frequency. Climate models produce contrasting projections due to different relative importance of ENSO feedback processes, different patterns of changes in the mean climate, as well as different depictions of decadal variability (e.g., Collins et al. 2010; DiNezio et al. 2012; Kim et al. 2014a; Chen et al. 2017). The power spectra of ENSO SST variability also exhibit large discrepancies across models and paleo reconstructions (Hope et al. 2017). However, there is a better inter-model consensus on a general increase in ENSO-driven tropical rainfall in the equatorial central and eastern Pacific in response to global warming, reflecting the consensus for more mean warming in the eastern equatorial Pacific (Power et al. 2013; Chung et al. 2014).

According to CMIP5 scenario simulations, the projected weakening of the Walker Circulation in the 21st century (e.g., Vecchi et al. 2006; Kociuba and Power 2014) with faster warming in the eastern equatorial Pacific than in the surrounding oceans is expected to shift

atmospheric convection into this usually cold and dry region, resulting in more occurrences of heavy precipitation that characterize an extreme El Niño (Cai et al. 2014). The projection does not arise from the climatological increase in mean rainfall and is robust when using atmospheric vertical velocity (Cai et al. 2017). The associated weakening of the climatological equatorial ocean currents is expected to promote eastward propagating SST anomalies – a characteristic of the 1982/83 and 1997/98 extreme El Niño events (Santoso et al. 2013). On the other hand, increased occurrences of extreme La Niña events characterized by anomalous surface cooling in Central Pacific could also arise due to faster warming of the Maritime Continent and eastern Pacific than the Central Pacific (Cai et al. 2015b). The warming background climate can enhance ENSO teleconnection and thus its impact, even if the SST anomalies themselves do not intensify (Cai et al. 2015a; Power et al. 2018). Even if global warming is kept below 1.5°C or 2°C, the risk associated with increased extreme El Niño frequency and ENSO-related major rainfall disruptions is likely to persist or even increase (Wang et al. 2017; Power et al. 2017a). In fact, global warming might have already made ENSO events more disruptive (Power et al. 2017a), enhancing ENSO-driven variability in many regions around the world (Bonfils et al. 2015; Power et al. 2018).

These projections may be sensitive to model deficiencies in simulating ENSO. As shown by Vijayeta and Dommenges (2017) using the recharge oscillator framework, models tend to underestimate ENSO feedback processes. Realistic simulation of ENSO behavior may stem from error-compensation rather than from correct simulation of the governing feedback processes. Confidence in projections is also reduced by the inability of climate models to capture decadal 'La Niña-like' trends as strong as those observed in the Pacific in recent decades (e.g., Kociuba and Power 2014; England et al. 2014), and a tendency to overestimate Pacific warming over the past 50 years (Power et al. 2017b). Possible reasons include model underestimation of internal variability (Kociuba and Power 2014; Power et al. 2017b), biases

in the upper ocean thermal stratification (Kohyama et al. 2017), as well as biases in the inter-basin warming contrast across the three oceans and in the SST-cloud forcing feedback (Luo et al. 2018). To reduce uncertainty in ENSO future projections, it is clear that much work needs to be done to improve climate models.

2.4. ENSO modelling

Poor simulation of ENSO is often linked to the persistent 'cold-tongue' bias in which the cold upwelled water in the eastern equatorial Pacific extends too far west toward the Maritime Continent (Fig. 4a). A "double Intertropical Convergence Zone (ITCZ)" is also associated with this cold tongue bias. These biases can affect ENSO simulation through misrepresentation of air-sea feedbacks (Kim et al. 2014b; Wengel et al. 2018). Graham et al. (2017) showed that the cold tongue bias leads to a propensity for occurrences of spatially double-peaked ENSO SST anomalies (peaking concurrently in both the eastern and central Pacific), which are not apparent in historical observations.

Another important ENSO feature is its synchronisation to the annual cycle, with peak SST anomalies typically occurring during austral summer. However, many models still do not represent this accurately (Fig. 4b). Worse, in some models (such as those highlighted in Fig. 4b) the seasonality is completely reversed (Taschetto et al. 2014). A suite of important processes shapes ENSO seasonality and the incorrect seasonality indicates that the underlying ENSO dynamics (e.g., SST-cloud and thermocline feedbacks) in the models are unlikely to be correct (Rashid and Hirst 2016). This, together with the bias in anomaly patterns, has ramifications for determining ENSO teleconnections and predicting ENSO impacts on rainfall, for instance.

How these unrealistic ENSO features affect future projections needs to be carefully considered and investigated through detailed analysis of the underlying coupled feedbacks (e.g., Guilyardi et al. 2016; Capotondi et al. 2015b), which are also dependent upon the mean state. As an example, Rashid et al. (2016) found that the strengths of the zonal wind stress forcing and wind-convection coupling simulated by the CMIP5 models largely determine whether the ENSO amplitude will increase or decrease under global warming in those models. Importantly, improvement of the model's mean state is critical. For instance, by taking into account the effect of ocean currents on the momentum transfer to the atmosphere (Pacanowski 1987), Luo et al. (2005) found a notable reduction in the cold tongue bias in their climate model.

The equatorial Pacific cold tongue is also affected by small-scale oceanic processes such as tropical instability waves (TIWs). TIWs are not well resolved by current state-of-the-art climate models which are still run at relatively coarse ocean resolution. TIWs heat the Pacific cold tongue at a rate comparable to atmospheric heating (up to 1°C/month; e.g., Menkes et al. 2006) and can potentially be an important nonlinear negative feedback on ENSO (An and Jin 2004). Research into TIWs influence on ENSO is still limited. Holmes et al. (2018) address how TIWs modify the response of the Central and Eastern Pacific to WWBs, providing a first estimate of TIWs contribution to ENSO irregularity, with implications for ENSO prediction (also see Ham and Kang 2011).

In addition, the Pacific cold tongue is a region of strong atmospheric heat uptake, and vigorous turbulent mixing that transports this heat into the ocean interior. Recent research by Holmes et al. (in preparation) has highlighted the global significance of air-sea fluxes and turbulent mixing in this region for modulating ocean heat uptake. However, the parameterization of this vertical mixing in climate models remains a difficult task, and

improvements are required in order to reduce model biases (e.g., Sasaki et al. 2013; Zhu and Zhang 2018).

2.5. Low frequency variability

ENSO properties vary on decadal and longer time scales (e.g., Holbrook et al. 2014; Wittenberg 2015; Power and Smith 2007) through changes in air-sea feedbacks linked to noise, chaotic dynamics, and slow variations in the mean state (e.g., Wittenberg 2009; Newman et al. 2011; Wittenberg et al. 2014; Zhao et al. 2016). While the mean-state variations are thought to be in part a rectified effect of changes in ENSO (e.g., Power and Colman 2006; Ogata et al. 2013), they also affect the interactions between ENSO and other modes of variability such as the SAM (e.g. Lim et al. 2016), as well as their eventual impact, such as on atmospheric cyclones and anticyclones. It is therefore crucial to understand the processes governing mean-state changes and their impact on ENSO.

The impact of mean-state change was highlighted by the 1970s climate shift that saw the Pacific climate system transition into a positive IPO that lasted until the late 1990s. Since then, the issue has been reignited by the recent short-lived slowdown in global surface warming that coincided with a negative IPO phase (approx. 1999-2012). In contrast to the preceding positive IPO, this negative IPO period was marked by a lack of strong El Niño, more frequent Central Pacific El Niños, more prominent La Niñas (e.g., see Fig. 3 of Santos et al. 2017), and reduced seasonal predictability (Zhao et al. 2016). This change in ENSO characteristics and predictability was attributed by Zhao et al. (2016) to reduction in the strength of the Bjerknes feedback in the central and eastern Pacific as a result of the IPO-related colder surface temperatures and enhanced mean Walker Circulation.

The IPO can be partially explained as the accumulated response to interdecadal variability in ENSO activity (Power et al. 2006; Newman et al. 2016). However, other factors may be involved, and the extent to which the IPO influences ENSO activity requires further study. More research is needed into the processes governing decadal variability, including those during the slowdown period as well as periods of more rapid warming. For instance, the cause for the unprecedented strength of the Pacific Trade Winds during the global warming hiatus period (England et al. 2014) needs to be better understood, including the roles of interbasin warming contrast, radiative forcing, and ENSO rectification onto the mean-state. Modelling studies have shown that these factors can influence the strength of Pacific climate change (e.g., Luo et al. 2018; Kohyama et al. 2017).

Recent studies indicate that warming trends in other ocean basins could be the cause for the record strong Pacific trade winds during 1999-2012. In particular, the role of the Atlantic warming trend appears to be important (e.g., McGregor et al. 2014; Luo et al. 2017). Models tend to underestimate the recent Pacific wind acceleration and to have strong climatological biases in the Atlantic Ocean. Indeed, there is an inter-model relationship between these two aspects (Kajtar et al. 2017; McGregor et al. 2018), highlighting the need to account for other basins in studying Pacific decadal variability.

In addition, using an eddy-permitting ocean model, Maher et al. (2017) showed that the recent Pacific Trade Wind acceleration can explain heat content trends in the Pacific Ocean, and in the Indian Ocean via the Indonesian Throughflow. They also showed that these heat content anomalies do not entirely dissipate with the abatement of the Pacific winds, leaving residual heat in the ocean. The impact of low-frequency subduction of heat on ENSO processes, particularly over decadal timescales, warrants further investigation.

3. Summary and closing remarks

The following key issues were raised during the workshop:

- **Characteristics of ENSO extremes:** The 2015/16 El Niño demonstrated potential diversity in extreme El Niño events than previously realized. It highlights the need for a better understanding of the causes and predictability of extreme ENSO events, supported by high-quality observational data and metrics toward better monitoring, predicting, and analyzing future events.
- **ENSO predictability:** There is scope to improve our understanding of ENSO development and ENSO representation in climate models, toward better operational predictive capability. Other than WWV and WWBs, climate variability and trends outside the tropical Pacific are also important factors. Decadal variability and long-term changes of these factors have important implications for the decadal predictability of ENSO.
- **Response to greenhouse forcing:** There is an indication that extreme ENSO events may become more frequent in a warmer future, and the present global warming may already be great enough to exacerbate the ENSO-induced rainfall disruption in the Pacific. Given existing model biases, there is a need to continually revise these assessments with improved models (e.g., CMIP6).
- **Model bias:** Current state-of-the-art climate models still have problems simulating the detailed nuances of ENSO and its seasonality, and these problems may be linked to the persistent cold tongue bias and its broader effects (e.g., double ITCZ bias) as well as biases in other basins that can impact ENSO through atmospheric and oceanic teleconnections.

- **Synoptic-scale oceanic processes:** Tropical instability waves, which are not well resolved in climate models, are an under-represented source of ocean mixing. Our understanding of ENSO irregularity would benefit from quantifying the relative effects of ocean noise and atmospheric stochasticity.
- **Mechanisms for decadal variability and trends:** Further research is needed to clarify the manner in which the IPO and other aspects of decadal variability interact with ENSO, and the extent to which the IPO is attributed to red noise associated with ENSO and other factors including external forcing and the role of remote oceanic basins.

The key elements of our discussions are summarized in Figure 5 which highlights areas of challenges and the ramifications associated with understanding ENSO dynamics and predictability. While ENSO predictability and the regional impacts can vary across events and decades (e.g., Power et al. 1999; Barnston et al. 2012; Karamperidou et al. 2014; Zhao et al. 2016) and ENSO predictability limit is not yet known (e.g., Newman and Sardeshmukh 2017), improved understanding of the interaction of these processes and their depiction in climate models could ultimately improve seasonal forecasts, decadal predictions, and future projections of ENSO. This should also lead to more accurate identification of ENSO impacts, with longer lead times and potential benefits to improved climate risk management. These are especially important for Australia given the pronounced and complex ENSO impacts on its regional climate (section 1), but this should also be applicable to all other ENSO-affected countries. The way forward is to sustain and expand ENSO research through further advances in modelling, observations, theoretical frameworks, forecasts, analysis techniques, and development of new metrics/indices, coordinated across a collaborative international research environment.

479 Such endeavors have been ongoing in Australia and nurtured by various government
480 initiatives, organizations, universities, and industries. Research collaboration and student
481 training across institutions are fostered through, for example, the currently active National
482 Environmental Science Program (www.environment.gov.au/science/nesp), and the Australian
483 Research Council (ARC) Centre of Excellence for Climate Extremes
484 (<http://climateextremes.org.au>), both of which integrate various ENSO related topics within
485 their overarching research programs. The ARC Centre has extended the collaborative
486 network to include several international institutions. ENSO is a core research element in the
487 recently established Centre for Southern Hemisphere Oceans Research (CSHOR;
488 <http://cshor.csiro.au>), which is a partnership between the CSIRO and Qingdao National
489 Laboratory for Marine Science and Technology (QNLN), with UNSW and University of
490 Tasmania as partners.

491 Australia has the National Computational Infrastructure (NCI) that provides high-
492 performance computing and data intensive services to researchers, supporting model
493 development such as Australia's national climate model, the Australian Community Climate
494 and Earth System Simulator (ACCESS) that contributes to CMIP and IPCC. The
495 development of ACCESS has involved close international partnerships, particularly with the
496 UK Met Office (UKMO) and the US Geophysical Fluid Dynamics Laboratory (GFDL).

497 The seasonal forecast system that is used to produce ENSO outlook continues to advance at
498 the Bureau, with POAMA to be replaced in 2018 by the seasonal forecast version of
499 ACCESS (ACCESS-S) which is of a higher resolution and better than POAMA in
500 distinguishing between EP and CP El Niño events, particularly at increasing lead times
501 (Hudson et al. 2017). Development and improvement of the Bureau's coupled model
502 predictions systems rely heavily on the partnership with the UKMO, but have also been and

continue to be strongly supported by various agricultural research and development corporations with matching funding from the Australian Government through the Managing Climate Variability Program (<http://managingclimate.gov.au>). Some of the key focus of the Bureau's research directions toward improved seasonal predictions include tackling key model biases that are affecting the simulation and prediction of ENSO diversity, improving data assimilation techniques for more accurate forecast model initialization, extending ENSO prediction lead times, and exploring the potential for multi-year prediction of ENSO.

Observing the tropical Pacific for ENSO, of which the TAO/TRITON mooring arrays (www.pmel.noaa.gov/gtmmba) have been instrumental, is an integral part of international effort in ocean observations under the auspices of Global Ocean Observing System (GOOS). While not a contributor to TAO/TRITON, Australia is a major contributor to GOOS through deployment of Argo floats operated by the Integrated Marine Observing System (IMOS; imos.org.au). The global array of Argo profiling floats provides real-time data of temperature, salinity, and currents up to 2000-m depth over the global oceans including the tropical Pacific. The Bureau relies on Argo subsurface temperature and salinity data for initializing their seasonal prediction models.

Australian ENSO researchers have also actively participated in international initiatives and organizations, such as the World Climate Research Program, TPOS 2020, IPCC, among many others, that in turn foster and enrich ENSO research activities. The future success of ENSO research and prediction in Australia will certainly benefit from sustained cross-institutional synergies in a conducive environment of the multi-national network.

Acknowledgments

The authors thank the Australian Research Council (ARC) Centre of Excellence for Climate System Science and the ARC Centre of Excellence for Climate Extremes for supporting the workshop. The workshop stemmed in part from discussions at a meeting of the National Environmental Science Program (NESP) Earth System and Climate Change Hub Project 2.2 science team. Andrew Wittenberg and two anonymous reviewers provided constructive comments and suggestions that improved the manuscript. The writing of this essay is partly supported by NESP, and Centre for Southern Hemisphere Oceans Research (CSHOR), a joint research centre for Southern Hemisphere ocean research between QNLM and CSIRO.

References

- Abellán, E., S. McGregor, M. H. England, and A. Santoso, 2017: Distinctive role of ocean advection anomalies in the development of the extreme 2015–16 El Niño, *Climate Dynamics*. <https://doi.org/10.1007/s00382-017-4007-0>
- Ashok, K., S. K. Behera, S. A. Rao, H. Weng, and T. Yamagata, 2007: El Niño Modoki and its possible teleconnection. *J. Geophysical Research*, **112**, C11007. <https://doi.org/10.1029/2006JC003798>
- An, S. and F.-F. Jin, 2004: Nonlinearity and Asymmetry of ENSO, *J. Climate*, **17**, 2399–2412.
- Bjerknes, J., 1969: Atmospheric teleconnections from the equatorial Pacific. *Mon Wea. Rev.*, **97**, 163–172.
- Bonfils, C.J., B.D. Santer, T.J. Phillips, K. Marvel, L.R. Leung, C. Doutriaux, and A. Capotondi, 2015: Relative Contributions of Mean-State Shifts and ENSO-Driven Variability to Precipitation Changes in a Warming Climate. *J. Climate*, **28**, 9997–10013, <https://doi.org/10.1175/JCLI-D-15-0341.1>

550 Barnston, A. G., et al., 2012: Skill of Real-Time Seasonal ENSO Model Predictions during
551 2002–11: Is Our Capability Increasing?. *Bull. Amer. Meteor. Soc.*, **93**, 631–651, doi:
552 10.1175/BAMS-D-11-00111.1

553 Blunden, J., and D. S. Arndt, Eds., 2016: State of the Climate in 2016. *Bull. Amer. Meteor.*
554 *Soc.*, **98** (8), Si–S277, doi:10.1175/2017BAMSSStateoftheClimate.1.

555 Cai, W., P. van Rensch, T. Cowan, and H.H. Hendon, 2011: Teleconnection Pathways of
556 ENSO and the IOD and the Mechanisms for Impacts on Australian Rainfall. *J.*
557 *Climate*, **24**, 3910–3923, <https://doi.org/10.1175/2011JCLI4129.1>

558 Cai, W. et al., 2014: Increasing frequency of extreme El Niño events due to greenhouse
559 warming. *Nature Climate Change*, **4**, 111–116, doi:10.1038/nclimate2100

560 Cai, W. et al., 2015a: ENSO and greenhouse warming, *Nature Climate Change*, **5**, 849–859,
561 doi:10.1038/nclimate2743

562 Cai, W., et al., 2015b: Increased frequency of extreme La Niña events under greenhouse
563 warming. *Nature Climate Change*, **5**, 132–137, doi:10.1038/nclimate2492

564 Cai, W., G. Wang, A. Santoso, X. Lin, and L. Wu, 2017: Definition of extreme El Niño and
565 its impact on projected increase in extreme El Niño frequency. *Geophysical Research Letters*,
566 **44**, 11,184–11,190. <https://doi.org/10.1002/2017GL075635>

567 Capotondi, A., et al., 2015a: Understanding ENSO diversity. *Bull. Amer. Met. Soc.*, **96**, 921–
568 938. doi: 10.1175/BAMS-D-13-00117.1

569 Capotondi, A., et al., 2015b: Climate model biases and El Niño Southern Oscillation (ENSO)
570 simulation. *U.S. CLIVAR Variations*, **13** (1), 21–25.

571 Chen, C., et al., 2017: ENSO in the CMIP5 simulations: Life cycles, diversity, and responses
572 to climate change. *J. Climate*, 30 (2), 775–801. doi: 10.1175/JCLI-D-15-0901.1

573 Chung, C.T.Y., S. B. Power, J. M. Arblaster, H. A. Rashid and G. L. Roff, 2014: Nonlinear
574 precipitation response to El Niño and global warming in the Indo-Pacific, *Climate Dynamics*,
575 **42**, 1837–1856, 10.1007/s00382-013-1892-8.

576 Chung, C.Y.Y., and S. B. Power, 2017: The non-linear impact of El Nino, La Nina and the
577 Southern Oscillation on seasonal and regional Australian precipitation. *J. Southern*
578 *Hemisphere Earth System Sci.*, **67**, 25-45. DOI: 10.22499/3.6701.003.

579 Collins, M. et al., 2010: The impact of global warming on the tropical Pacific Ocean and El
580 Niño, *Nature Geoscience*, **3**, 391–397, doi:10.1038/ngeo868.

581 DiNezio, P., et al., 2012: Mean climate controls on the simulated response of ENSO to
582 increasing greenhouse gases. *J. Climate*, **25**, 7399-7420. doi: 10.1175/JCLI-D-11-00494.1

583 Dommenges, D., T. Bayr, and C. Frauen, 2013: Analysis of the non-linearity in the pattern
584 and time evolution of El Niño Southern Oscillation. *Climate Dynamics*, **40**(11-12), 2825–
585 2847. <https://doi.org/10.1007/s00382-012-1475-0>

586 Dong, L., and M. J. McPhaden, 2018: Unusually warm Indian Ocean sea surface
587 temperatures help to arrest development of El Niño in 2014. *Scientific Rep.*, **8**, 2249, doi:
588 10.1038/s41598-018-20294-4

589 Drosowsky, W. and L.E. Chambers, 2001: Near-Global Sea Surface Temperature
590 Anomalies as Predictors of Australian Seasonal Rainfall. *J. Climate*, **14**, 1677–1687,
591 doi:10.1175/1520-0442(2001)014<1677:NACNGS>2.0.CO;2

592 England et al., 2014: Recent intensification of wind-driven circulation in the Pacific and the
593 ongoing warming hiatus, *Nature Climate Change*, **4**, 222–227, doi:10.1038/nclimate2106.

594 Graham, F. S., J. N. Brown, A. T. Wittenberg, S. J. Marsland, and N. J. Holbrook, 2017:
595 Understanding the double peaked El Niño in coupled GCMs. *Climate Dynamics*, **48**, 2045-
596 2063, doi:10.1007/s00382-016-3189-1.

597 Guilyardi, E., et al., 2016: Fourth CLIVAR Workshop on the Evaluation of ENSO Processes
598 in Climate Models: ENSO in a Changing Climate. *Bull. Amer. Meteor. Soc.*, **97** (5), 817-820.
599 doi: 10.1175/BAMS-D-15-00287.1

600 Ham, Y.-G., and I.-S. Kang, 2011: Improvement of seasonal forecasts with inclusion of
601 tropical instability waves on initial conditions. *Climate Dynamics*, **36**, 1277-1290.

602 Hannam, P., 2014: “Most-watched” El Niño gathers pace in the Pacific. Sydney Morning
 603 Herald. [http://www.smh.com.au/environment/weather/mostwatched-el-Niño-gathers-pace-in-](http://www.smh.com.au/environment/weather/mostwatched-el-Niño-gathers-pace-in-pacific-20140617-zsaw6.html)
 604 [pacific-20140617-zsaw6.html](http://www.smh.com.au/environment/weather/mostwatched-el-Niño-gathers-pace-in-pacific-20140617-zsaw6.html)

605 Hendon, H., D. Thompson, and M. Wheeler, 2007: Australian rainfall and surface
 606 temperature variations associated with the southern annular mode. *J. Climate*, **20**, 2452–
 607 2467.

608 Hendon, H. H., E. Lim, G. Wang, O. Alves and D. Hudson, 2009: Prospects for predicting
 609 two flavors of El Nino. *Geophys. Res. Lett.*, **36**, L19713, doi:10.1029/2009GL040100.

610 Hendon, H. H., E.-P. Lim, and G. Liu, 2012: The Role of Air–Sea Interaction for Prediction
 611 of Australian Summer Monsoon Rainfall. *J. Climate*, **25**, 1278–1290,
 612 <https://doi.org/10.1175/JCLI-D-11-00125.1>

613 Henley, B., et al., 2016: A tripole index for the Interdecadal Pacific Oscillation. *Climate*
 614 *Dyn.*, **45**, 3077-3090.

615 Holbrook, N. J., J. Li, M. Collins, E. Di Lorenzo, et al., 2014: Decadal climate variability and
 616 cross-scale interactions: ICCL 2013 Expert Assessment Workshop. *Bulletin of the American*
 617 *Meteorological Society*, **95**, ES155-ES158. doi: 10.1175/BAMS-D-13-00201.1.

618 Holbrook, N. J., J. Davidson, M. Feng, A. J. Hobday, J. M. Lough, S. McGregor, and J. S.
 619 Risbey, 2009: Chapter 4: El Niño – Southern Oscillation. In *Report Card of Marine Climate*
 620 *Change for Australia: detailed scientific assessment*, Eds. E. S. Poloczanska, A. J. Hobday
 621 and A. J. Richardson, NCCARF Publication 05/09, pp.29-51, ISBN 978-1-921609-03-9.

622 Holmes, R. M., S. McGregor, A. Santoso, and M. H. England, 2018: Contribution of Tropical
 623 Instability Waves to ENSO Irregularity. *Climate Dynamics*, [https://doi.org/10.1007/s00382-](https://doi.org/10.1007/s00382-018-4217-0)
 624 [018-4217-0](https://doi.org/10.1007/s00382-018-4217-0)

625 Hope, P., B. J. Henley, J. Gergis, et al., 2017: Time-varying spectral characteristics of ENSO
 626 over the Last Millennium, *Climate Dynamics*, **49**, 1705. [https://doi.org/10.1007/s00382-016-](https://doi.org/10.1007/s00382-016-3393-z)
 627 [3393-z](https://doi.org/10.1007/s00382-016-3393-z)

628 Huang, B., P. Thorne, V. Banzon, T. Boyer, et al., 2017: Extended reconstructed sea surface
629 temperature version 5 (ERSSTv5): Upgrades, validations, and intercomparisons. *Journal of*
630 *Climate*, **30**(20), 8179–8205. <https://doi.org/10.1175/JCLI-D-16-0836.1>

631 Hu, S., and A. V. Fedorov, 2016: Exceptionally strong easterly wind burst stalling El Niño of
632 2014. *PNAS*, **113**(8), 2005–2010. doi:10.1073/pnas.1514182113

633 Hudson, D., et al. 2017: ACCESS-S1: The new Bureau of Meteorology multi-week to
634 seasonal prediction system. *J. Southern Hemisphere Earth Systems Science*, **67** (3), 132-159.

635 Ishii, M, A. Shouji, S. Sugimoto, and T. Matsumoto, 2005: Objective analyses of sea-surface
636 temperature and marine meteorological variables for the 20th century using ICOADS and the
637 Kobe collection, *Int. J. Climatology*, **25**(7), 865-879.

638 Jin, F.-F., 1997: An equatorial ocean recharge paradigm for ENSO. Part I: Conceptual
639 model. *Journal of the Atmospheric Sciences*, **54**(7), 811–829. [https://doi.org/10.1175/1520-](https://doi.org/10.1175/1520-0469(1997)054%3C0811:AEORPF%3E2.0.CO;2)
640 [0469\(1997\)054%3C0811:AEORPF%3E2.0.CO;2](https://doi.org/10.1175/1520-0469(1997)054%3C0811:AEORPF%3E2.0.CO;2)

641 Kajtar, J. B., A. Santoso, S. McGregor, and M. H. England, 2017: Model under-
642 representation of decadal Pacific trade wind trends and its link to tropical Atlantic bias.
643 *Climate Dynamics*, <https://doi.org/10.1007/s00382-017-3699-5>

644 Kalnay, K., et al., 1996: The NCEP/NCAR 40-year reanalysis project. *Bulletin of the*
645 *American Meteorological Society*, **77**(3), 437–471. [https://doi.org/10.1175/1520-](https://doi.org/10.1175/1520-0477(1996)077%3C0437:TNYRP%3E2.0.CO;2)
646 [0477\(1996\)077%3C0437:TNYRP%3E2.0.CO;2](https://doi.org/10.1175/1520-0477(1996)077%3C0437:TNYRP%3E2.0.CO;2)

647 Kao, H.-Y., and J.-Y. Yu, 2009: Contrasting eastern Pacific and central Pacific types of El
648 Niño. *J. Climate*, **22**, 615–632.

649 Karamperidou, C., et al., 2014: Intrinsic modulation of ENSO predictability viewed through a
650 local Lyapunov lens. *Climate Dyn.*, **42**, 253-270. doi: 10.1007/s00382-013-1759-z

651 Kim, S.-T., W. Cai, F.-F. Jin, A. Santoso, L. Wu, E. Guilyardi, S.-I. An, 2014a: Response of
652 El Niño sea surface temperature variability to greenhouse warming. *Nature Climate Change*,
653 **4**, 786-790.

654 Kim, S.-T., W. Cai, F.-F. Jin, and J.-Y. Yu, 2014b: ENSO stability in coupled climate models
655 and its association with mean state. *Clim. Dyn.*, **42**, 3313–3321. doi: 10.100/s0382-013-1833-
656 6

657 Kohyama, T., D. L. Hartmann, and D. S. Battisti, 2017: La Niña–like mean-state response to
658 global warming and potential oceanic roles. *J. Climate*, **30**, 4207–4225,
659 <https://doi.org/10.1175/JCLI-D-16-0441.1>

660 Lee, S.-K., et al., 2014: Spring persistence, transition and resurgence of El Niño. *Geophys.*
661 *Res. Lett.*, **41** (23), 8578–8585. doi: 10.1002/2014GL062484

662 Levine, A. F. Z., and McPhaden, M. J., 2016: How the July 2014 easterly wind burst gave the
663 2015–2016 El Niño a head start. *Geophysical Research Letters*, **43**, 6503–6510.
664 <https://doi.org/10.1002/2016GL069204>

665 L’Heureux, M. L., K. Takahashi, A. B. Watkins, A. G. Barnston, E. J. Becker, et al., 2017:
666 Observing and predicting the 2015/16 El Niño. *Bulletin of the American Meteorological*
667 *Society*, **98**(7), 1363–1382. <https://doi.org/10.1175/BAMS-D-16-0009.1>

668 Lim, E.-P. and H. H. Hendon 2015: Understanding the contrast of Australian springtime
669 rainfall of 1997 and 2002 in the frame of two flavors of El Niño *J. Climate.*, **28**, 2804–2822

670 Lim, E.-P. and H. Hendon, 2017: Causes and predictability of the negative Indian Ocean
671 Dipole and its impact on La Niña during 2016. *Scientific Reports*, **7**, 12619
672 doi:10.1038/s41598-017-12674-z

673 Lim, E.-P., H. H. Hendon, J. M. Arblaster, C. Chung, A. F. Moise, P Hope, G. Young and M.
674 Zhao, 2016: Interaction of the recent 50 year SST trend and La Niña 2010: amplification of
675 the Southern Annular Mode and Australian springtime rainfall. *Climate Dynamics*, **47**, 2273–
676 2291.

677 Loughran, T. F., S. E. Perkins-Kirkpatrick, and L. V. Alexander, 2017: Understanding the
678 spatio-temporal influence of climate variability on Australian heatwaves. *Int. J. Climatol.*, **37**,
679 3963–3975. doi:10.1002/joc.4971

680 Lu, L., and D. Hedley, 2004: The impact of the 2002–03 drought on the economy and
681 agricultural employment. Economic Roundup Autumn 2004, The Treasury, Australian
682 Government, 25–44. [Available online at [http://www.treasury.gov.au/](http://www.treasury.gov.au/documents/817/PDF/roundup_autumn_2004.pdf)
683 [documents/817/PDF/roundup_autumn_2004.pdf](http://www.treasury.gov.au/documents/817/PDF/roundup_autumn_2004.pdf).]

684 Luo, J.-J., G. Liu, H. Hendon, O. Alves, and T. Yamagata, 2017: Inter-basin sources for two-
685 year predictability of the multi-year La Niña event in 2010–2012. *Scientific Reports*, **7**, 2276.
686 <http://doi.org/10.1038/s41598-017-01479-9>

687 Luo, J.-J., G. Wang, and D. Dommenges, 2018: May common model biases reduce
688 CMIP5’s ability to simulate the recent Pacific La Niña-like cooling? *Climate Dyn.*, **50**, 1335.
689 <https://doi.org/10.1007/s00382-017-3688-8>

690 Luo, J., S. Masson, E. Roeckner, G. Madec, and T. Yamagata, 2005: Reducing Climatology
691 Bias in an Ocean–Atmosphere CGCM with Improved Coupling Physics. *J.*
692 *Climate*, **18**, 2344–2360, <https://doi.org/10.1175/JCLI3404.1>

693 Maher, N., M. H. England, A. Sen Gupta, et al., 2017: Role of Pacific trade winds in driving
694 ocean temperatures during the recent slowdown and projections under a wind trend reversal,
695 *Climate Dynamics*, <https://doi.org/10.1007/s00382-017-3923-3>

696 McBride, J. L., and N. Nicholls, 1983: Seasonal relationship between Australian rainfall and
697 Southern Oscillation. *Mon. Wea. Rev.*, **111**, 1998–2004.

698 McGregor, S., A. Timmermann, M. F. Stuecker, M. H. England, M. Merrifield, F.-F. Jin, and
699 Y. Chikamoto, 2014: Recent Walker circulation strengthening and Pacific cooling amplified
700 by Atlantic warming, *Nature Climate Change*, **4**, 888–892, doi:10.1038/nclimate2330

701 McGregor, S., M. F. Stuecker, J. B. Kajtar, M. H. England, and M. Collins, 2017: Model
702 tropical Atlantic biases underpin diminished Pacific decadal variability, *Nature Climate*
703 *Change*, **8**, 493–498, <https://doi.org/10.1038/s41558-018-0163-4>.

704 McPhaden, M. J., 2015: Playing hide and seek with El Niño. *Nature Climate Change*, **5**(9),
705 791–795. <https://doi.org/10.1038/nclimate2775>

706 Meinen, C. S., and M. J. McPhaden, 2000: Observations of warm water volume changes in
707 the equatorial Pacific and their relationship to El Niño and La Niña. *J. Climate*, **13**(30),
708 3551-3559.

709 Menkes, C. et al., 2014: About the role of the westerly wind events in the possible
710 development of an El Niño in 2014. *Geophys. Res. Lett.*, **41**, 6476-6483, doi:
711 10.1002/2014GL061186

712 Menkes, C. et al., 2006: A modeling study of the impact of tropical instability waves on the
713 heat budget of the eastern equatorial Pacific. *J. Phys. Oceanogr.*, **36**, 847-865.

714 Meyers, G., P. McIntosh, L. Pigot, and M. Pook, 2007: The years of El Niño, La Niña, and
715 interactions with the tropical Indian Ocean. *J. Climate*, **20**, 2872–2880.

716 Neske, S., and S. McGregor, 2018: Understanding the warm water volume precursor of
717 ENSO events and its interdecadal variation. *Geophysical Research Letters*, **45**.
718 <https://doi.org/10.1002/2017GL076439>

719 Newman, M., S.-I. Shin, and M. A. Alexander, 2011: Natural variation in ENSO flavors.
720 *Geophys. Res. Lett.*, **38**, L14705, doi: 10.1029/2011GL047658

721 Newman, M., et al., 2016: The Pacific Decadal Oscillation, Revisited. *J. Climate*, **29**, 4399–
722 4427, <https://doi.org/10.1175/JCLI-D-15-0508.1>

723 Newman, M., et al., 2018: The extreme 2015/16 El Niño, in the context of historical climate
724 variability and change. [in “Explaining Extreme Events of 2016 from a Climate
725 Perspective”]. *Bull. Amer. Meteor. Soc.*, **99**, S16-S20, doi:10.1175/BAMS-D-17-0118.1.

726 Nicholls, N., 1984: The Southern Oscillation and Indonesian Sea Surface Temperature. *Mon.*
727 *Wea. Rev.*, **112**, 42 - 432, doi: 10.1175/15200493(1984)112<0424:TSOAI>2.0.CO;2

728 Nicholls, N., 1985: Impact of the Southern Oscillation on Australian crops. *J. Climatology*,
729 **5**, 553-560.

730 Nicholls, N., 1991: The El Nino/Southern Oscillation and Australian vegetation. *Vegetatio*,
731 **91**, 23-36.

732 Norman, F. I., and N. Nicholls, 1991: The Southern Oscillation and variations in waterfowl
 733 abundance in southeastern Australia. *Australian J. Ecology*, **16**, 485-490.

734 Ogata, T., et al., 2013: Interdecadal amplitude modulation of El Niño-Southern Oscillation
 735 and its impacts on tropical Pacific decadal variability. *J. Climate*, **26**, 7280-7297. doi:
 736 10.1175/JCLI-D-12-00415.1

737 Pacanowski, R., 1987: Effect of equatorial currents on surface stress. *J. Phys.*
 738 *Oceanogr.*, **17**, 833–838.

739 Paek, H., J.Y. Yu, and C. Qian, 2017: Why were the 2015/2016 and 1997/1998 extreme El
 740 Niños different? *Geophysical Research Letters*, **44**, 1848–1856. doi:10.1002/2016GL071515

741 Power, S. B., and I. N. Smith, 2007: Weakening of the Walker Circulation and apparent
 742 dominance of El Niño both reach record levels, but has ENSO really changed? *Geophys. Res.*
 743 *Lett.*, **34**, L18702, doi:10.1029/2007GL030854.

744 Power, S., Tseitkin, F., Torok, S., Lavery, B., and B. McAvaney, 1998: Australian
 745 temperature, Australian rainfall, and the Southern Oscillation, 1910-1996: Coherent
 746 variability and recent changes. *Aust. Meteorol. Mag.*, **47**, 85-101.

747 Power, S., Folland, C., Colman, A., and V. Mehta, 1999: Inter-decadal modulation of the
 748 impact of ENSO on Australia. *Climate Dynamics*, **15**, 319-324.

749 Power, S., F. Delage, C. Chung, G. Kociuba, and K. Keay, 2013: Robust twenty-first-century
 750 projections of El Niño and related precipitation variability, *Nature*, **502**, 541–545,
 751 doi:10.1038/nature12580

752 Power, S. B., F. P. D. Delage, C. T. Y. Chung, H. Ye, and B. F. Murphy, 2017a: Humans
 753 have already increased the risk of major disruptions to Pacific rainfall. *Nature*
 754 *Communications*, doi: 10.1038/ncomms14368.

755 Power, S., Delage, F., Wang, G. et al., 2017b: Apparent limitations in the ability of CMIP5
 756 climate models to simulate recent multi-decadal change in surface temperature: implications
 757 for global temperature projections, *Climate Dynamics*, **49**, 53.
 758 <https://doi.org/10.1007/s00382-016-3326-x>

759 Power, S.B. and J. Callaghan, 2016: Variability in Severe Coastal Flooding, Associated
760 Storms, and Death Tolls in Southeastern Australia since the Mid–Nineteenth Century. *J.*
761 *Appl. Meteor. Climatol.*, **55**, 1139–1149, <https://doi.org/10.1175/JAMC-D-15-0146.1>

762 Power, S.B., and R. Colman, 2006: Multi-year predictability in a coupled general circulation
763 model. *Climate Dynamics*, **26**, 247–272.

764 Power, S., M. Haylock, R. Colman, and X. Wang, 2006: The predictability of interdecadal
765 changes in ENSO and ENSO teleconnections. *J. Climate*, **8**, 2161–2180.

766 Power, S., and F.P.D. Delage, 2018: El Niño–Southern Oscillation and Associated Climatic
767 Conditions around the World during the Latter Half of the Twenty-First Century. *J. Climate*,
768 **31**, 6189–6207, <https://doi.org/10.1175/JCLI-D-18-0138.1>.

769 Pui, A., A. Sharma, A. Santoso, and S. Westra, 2012: Impact of the El Niño Southern
770 Oscillation, Indian Ocean Dipole, and Southern Annular Mode on daily to sub-daily rainfall
771 characteristics in East Australia. *Monthly Weather Review*, **140**, 1665–1682.

772 Puy, M., J. Vialard, M. Lengaigne, and E. Guilyardi, 2016: Modulation of equatorial Pacific
773 westerly/easterly wind events by the Madden-Julian Oscillation and convectively-coupled
774 Rossby waves. *Climate Dyn.*, **467**, 2155–2178.

775 Rashid, H. A., A. C. Hirst and S. Marsland, 2016: An atmospheric mechanism for ENSO
776 amplitude changes under an abrupt quadrupling of CO2 concentration in CMIP5 models.
777 *Geophysical Research Letters*, **43**, 1687–1694, doi:10.1002/2015GL066768.

778 Rashid, H. A., and A. C. Hirst, 2016: Investigating the mechanisms of seasonal ENSO phase
779 locking bias in the ACCESS Coupled Model. *Climate Dynamics*, **46**, 1075–1090.

780 Risbey, J.S., M.J. Pook, P.C. McIntosh, M.C. Wheeler, and H.H. Hendon, 2009: On the
781 Remote Drivers of Rainfall Variability in Australia. *Mon. Wea. Rev.*, **137**, 3233–
782 3253, <https://doi.org/10.1175/2009MWR2861.1>

783 Ropelewski, C.F. and M.S. Halpert, 1987: Global and Regional Scale Precipitation Patterns
784 Associated with the El Niño/Southern Oscillation. *Mon. Wea. Rev.*, **115**, 1606–
785 1626, [https://doi.org/10.1175/1520-0493\(1987\)115<1606:GARSPP>2.0.CO;2](https://doi.org/10.1175/1520-0493(1987)115<1606:GARSPP>2.0.CO;2)

786 Saji, N. H., B. N. Goswami, P. N. Vinayachandran, and T. Yamagata, 1999: A dipole mode
787 in the tropical Indian Ocean. *Nature*, **401**(6751), 360-363. <https://doi.org/10.1038/43854>.

788 Santoso, A., S. McGregor, F.-F. Jin, W. Cai, M. H. England, S.-I. An, M. McPhaden, E.
789 Guilyardi, 2013: Late-twentieth-century emergence of the El Niño propagation asymmetry
790 and future projections. *Nature*, **504**, 126-130.

791 Santoso, A., W. Cai, M. Collins, M. McPhaden, F.-F. Jin, E. Guilyardi, G. Vecchi, D.
792 Dommenget, G. Wang, 2015: ENSO Extremes and Diversity: Dynamics, Teleconnections,
793 and Impacts. *Bulletin of the American Meteorological Society*, **96**, 1969-1972.

794 Santoso, A., McPhaden, M. J., and Cai, W., 2017: The defining characteristics of ENSO
795 extremes and the strong 2015/2016 El Niño. *Reviews of Geophysics*, **55**, 1079–1129.
796 <https://doi.org/10.1002/2017RG000560>

797 Sasaki, W., K. J. Richards, and J.-J. Luo, 2013: Impact of vertical mixing induced by small
798 vertical scale structures above and within the equatorial thermocline on the tropical Pacific in
799 a CGCM. *Clim. Dyn.*, **41**, 443. <https://doi.org/10.1007/s00382-012-1593-8>

800 Sullivan, A., et al., 2016: Robust contribution of decadal anomalies to the frequency of
801 central-Pacific El Niño. *Scientific Reports*, **6**, 38540, doi:10.1038/srep38540

802 Takahashi, K., A. Montecinos, K. Goubanova, and B. Dewitte, B, 2011: ENSO regimes:
803 Reinterpreting the canonical and Modoki El Niño. *Geophysical Research Letters*, **38**,
804 L10704. <https://doi.org/10.1029/2011GL047364>

805 Takahashi, K., and B. Dewitte, 2016: Strong and moderate nonlinear El Niño regimes.
806 *Climate Dynamics*, **46**(5-6), 1627–1645. <https://doi.org/10.1007/s00382-015-2665-3>

807 Taschetto, A. S., and M. H. England, 2009: El Niño Modoki Impacts on Australian Rainfall.
808 *Journal of Climate*, **22**(11), 3167–3174. <http://doi.org/10.1175/2008JCLI2589.1>

809 Taschetto, A. S., Sen Gupta, A., Hendon, H. H., Ummenhofer, C. C., & England, M. H.
810 (2011). The Contribution of Indian Ocean Sea Surface Temperature Anomalies on Australian
811 Summer Rainfall during El Niño Events. *Journal of Climate*, **24**, 3734–3747.

812 Taschetto, A.S., A.S. Gupta, N.C. Jourdain, A. Santoso, C.C. Ummenhofer, and M.H.
 813 England, 2014: Cold Tongue and Warm Pool ENSO Events in CMIP5: Mean State and
 814 Future Projections. *J. Climate*, **27**, 2861–2885, <https://doi.org/10.1175/JCLI-D-13-00437.1>

815 Thompson, D. W. J., and J. M. Wallace, 2000: Annular modes in the extratropical circulation.
 816 Part I: month-to-month variability. *J. Climate*, **13**, 1000-1016.

817 Timmermann, A., et al., 2018: El Niño-Southern Oscillation complexity. *Nature*, **559**, 535-
 818 5545.

819 Trenberth, K. E., and D. P. Stepaniak, 2001: Indices of El Niño evolution. *Journal of*
 820 *Climate*, **14**(8), 1697–1701. [https://doi.org/10.1175/1520-](https://doi.org/10.1175/1520-0442(2001)014%3C1697:LIOENO%3E2.0.CO;2)
 821 [0442\(2001\)014%3C1697:LIOENO%3E2.0.CO;2](https://doi.org/10.1175/1520-0442(2001)014%3C1697:LIOENO%3E2.0.CO;2)

822 Ummenhofer, C. C., Sen Gupta, A., England, M. H., Taschetto, A. S., Briggs, P. R., &
 823 Raupach, M. R. (2015). How did ocean warming affect Australian rainfall extremes during
 824 the 2010/2011 La Niña event? *Geophysical Research Letters*, **42**(22), 9942–9951.
 825 <http://doi.org/10.1002/2015GL065948>.

826 van Rensch, P., A. J. E. Gallant, W. Cai, and N. Nicholls (2015), Evidence of local sea
 827 surface temperatures overriding the southeast Australian rainfall response to the 1997–1998
 828 El Niño, *Geophys. Res. Lett.*, **42**, 9449–9456, doi: 10.1002/2015GL066319.

829 Vecchi, G. A., and D. E. Harrison, 2000: Tropical Pacific sea surface temperature anomalies,
 830 El Niño, and equatorial westerly wind events. *J. Climate*, **13**, 1814–1830.

831 Vecchi, G. A., et al., 2006: Weakening of tropical Pacific atmospheric circulation due to
 832 anthropogenic forcing. *Nature*, **441**, 73- 76. doi: 10.1038/nature04744

833 Vijayeta, A., and D. Dommenges, 2017: An evaluation of ENSO dynamics in CMIP
 834 simulations in the framework of the recharge oscillator model. *Climate Dyn.*,
 835 <https://doi.org/10.1007/s00382-017-3981-6>

836 Voice, M.E. and F.J. Gauntlett, 1984: The 1983 Ash Wednesday Fires in Australia. *Mon.*
 837 *Wea. Rev.*, **112**, 584–590, [https://doi.org/10.1175/1520-](https://doi.org/10.1175/1520-0493(1984)112<0584:TAWFIA>2.0.CO;2)
 838 [0493\(1984\)112<0584:TAWFIA>2.0.CO;2](https://doi.org/10.1175/1520-0493(1984)112<0584:TAWFIA>2.0.CO;2)

839 Wang, G., and H. H. Hendon, 2007: Sensitivity of Australian Rainfall to Inter–El Niño
840 Variations. *J. Climate*, **20**, 4211–4226, <https://doi.org/10.1175/JCLI4228.1>

841 Wang, G., and H. H. Hendon, 2017: Why 2015 was a strong El Niño and 2014 was not,
842 *Geophys. Res. Lett.*, **44**(16), doi:10.1002/2017GL074244.

843 Wang, G., S.B. Power, and S. McGree, 2016: Unambiguous warming in the western tropical
844 Pacific primarily caused by anthropogenic forcing. *Int. J. Climatol.*, **36**, 933–944, doi:
845 10.1002/joc.4395.

846 Wang, G., W. Cai, B. Gan, L. Wu, A. Santoso, X. Lin, Z. Chen, and M. McPhaden,
847 2017: Continued increase of extreme El Niño frequency long after 1.5C warming
848 stabilization. *Nature Climate Change*, **7**, 568–572.

849 Watkins, A., 2015: BOM: We’re calling it, the 2015 El Niño is here. The Conversation,
850 <https://theconversation.com/bom-were-calling-it-the-2015-el-Niño-is-here-41598>

851 Webster, P. J., and S. Yang, 1992: Monsoon and ENSO: Selectively interactive systems.
852 *Quarterly Journal of the Royal Meteorological Society*, **118**(507), 877–926.
853 <https://doi.org/10.1002/qj.49711850705>

854 Wengel, C., M. Latif, W. Park, W. et al., 2018: Seasonal ENSO phase locking in the Kiel
855 Climate Model: The importance of the equatorial cold sea surface temperature bias. *Clim.*
856 *Dyn.*, **50**, 901. <https://doi.org/10.1007/s00382-017-3648-3>

857 Werner A., and N. J. Holbrook, 2011: A Bayesian forecast model of Australian region
858 tropical cyclone formation. *Journal of Climate*, **24**, 6114–6131,
859 DOI:10.1175/2011JCLI4231.1.

860 Williams, A. A. J., and D. J. Karoly, 1999: Extreme fire weather in Australia and the impact
861 of the El Nino-Southern Oscillation. *Aust. Meteor. Mag.*, **48**, 15–22.

862 Wittenberg, A., 2009: Are historical records sufficient to constrain ENSO simulations?
863 *Geophys. Res. Lett.*, **36**, L12702. doi: 10.1029/2009GL038710
864

865 Wittenberg, A., et al., 2014: ENSO modulation: Is it decadal predictability? *J. Climate*, **27**,
866 2667–2681. doi: 10.1175/JCLI-D- 13-00577.1

- Wittenberg, A., 2015: Low-frequency variations of ENSO. *U.S. CLIVAR Variations*, **13** (1), 26-31.
- Xie, P., and P. A. Arkin, 1997: Global precipitation: A 17-year monthly analysis based on gauge observations, satellite estimates, and numerical model outputs. *Bulletin of the American Meteorological Society*, **78**(11), 2539–2558. [https://doi.org/10.1175/1520-0477\(1997\)078%3C2539:GPAYMA%3E2.0.CO;2](https://doi.org/10.1175/1520-0477(1997)078%3C2539:GPAYMA%3E2.0.CO;2)
- Xue, Y., and A. Kumar, 2017: Evolution of the 2015/16 el Niño and historical perspective since 1979. *Science China Earth Sciences*, **60**(9), 1572–1588. <https://doi.org/10.1007/s11430-016-0106-9>
- Zhao, M., H. H. Hendon, O. Alves, G. Liu, and G. Wang, 2016: Weakened eastern Pacific El Niño predictability in the early twenty-first century. *Journal of Climate*, **29**(18), 6805–6822. <https://doi.org/10.1175/JCLI-D-15-0876.1>
- Zhu, Y. and R.-H. Zhang, 2018: An Argo-derived background diffusivity parameterization for improved ocean simulations in the tropical Pacific, *Geophys. Res. Lett.*, **45** (3), [doi:10.1002/2017GL076269](https://doi.org/10.1002/2017GL076269).

897 **Table 1.** Definitions of terms discussed in this article.

898

Terminology	Definition
Bjerknes feedback ^a	Positive air-sea coupled feedback along the equator in which a positive SST anomaly during an El Niño growth phase induces westerly wind anomalies that deepen the thermocline thereby reinforcing the positive SST anomaly, and the cycle continues taking El Niño to its peak. The converse occurs during a La Niña.
Interdecadal Pacific Oscillation (IPO) ^b	Ocean-atmosphere variability in the Pacific Ocean operating on 10-30 year time scales with a near-global pattern resembling that of El Niño and La Niña during its positive/warm and negative/cold phases, respectively. The IPO could be a long-term integration of various processes including interannual and decadal components of ENSO variability, stochastic air-sea fluxes, as well as other sources of low-frequency variability.
Indian Ocean Dipole (IOD) ^c	Year-to-year climate variability in the Indian Ocean that peaks in austral spring with its positive phase exhibiting a pool of anomalously cold sea surface off Java-Sumatra, and anomalously warm sea surface off Africa. Such pattern is associated with weaker Walker Circulation over the Indian Ocean, and often coincides, but not always, with a developing El Niño. The converse occurs during the negative phase and La Niña.
Southern Annular Mode (SAM) ^d	Vacillations in atmospheric pressure over extratropical Southern Hemisphere to Antarctica associated with stronger westerly wind at high latitudes and weaker westerlies at mid latitudes during its positive phase, and conversely during the negative phase.

Walker Circulation ^a	Large-scale zonal atmospheric circulation in the tropical Pacific marked by easterly winds blowing from the colder eastern Pacific toward the Western Pacific warm pool where warm air rises and moves eastward as it loses moisture before eventually descending in the eastern Pacific. The Walker Circulation weakens during an El Niño and strengthens during a La Niña, and the <i>Southern Oscillation</i> refers to the associated vacillation of atmospheric pressure in the tropical western and eastern Pacific.
Warm water volume (WWV) ^e	Volume of water above 20°C isotherm across the equatorial Pacific (5°S-5°N, 120°E-80°W) as a proxy of upper equatorial Pacific Ocean heat content. Anomalously high WWV around austral autumn is a necessary condition for an El Niño at the end of the year. The opposite is true for La Niña.
Westerly wind burst (WWB) ^f	Sustained west-to-east winds over the western and central equatorial Pacific, typically exceeding a certain threshold (e.g., 2 m s ⁻¹) and lasting more than a few days.

^a Bjerknes (1969)

^b Power et al. (1999), Newman et al. (2016), Henley et al. (2016)

^c Saji et al. (1999)

^d Thompson and Wallace (2000)

^e Meinen and McPhaden (2000)

^f Vecchi and Harrison (2000), Puy et al. (2016)

Figure captions

Figure 1. ENSO diversity over 1980-2017. (a) Eastern Pacific (EP) ENSO index (EPI) versus Central Pacific (CP) index (CPI) averaged over December-February (DJF) when ENSO events typically peak, where circle size corresponds to ENSO amplitude and the color indicates the type (EP, CP, EP/CP). (b)-(e) Composite of DJF SST anomalies for each type of ENSO events. (f) SST anomaly over the equatorial Pacific (averaged over 5°S–5°N) marked by different colors that signify event types in (a). The EPI and CPI are based on those of Sullivan et al. (2016), defined as $Ni\tilde{no}3 - 0.5 * Ni\tilde{no}4$ and $Ni\tilde{no}4 - 0.5 * Ni\tilde{no}3$, respectively (where the Niño indices are first normalized). Niño3 and Niño4 indices are SST anomalies averaged over (5°S–5°N, 150°W–90°W) and (5°S–5°N, 160°E–150°W), respectively. An arbitrary threshold (Thr) can be applied to the indices to classify each year into EP, CP, or a mix (EP/CP). In this case, 0.7 of the index standard deviation (sdev.) is used (dotted lines), with the 1982/83 and 1997/98 extreme El Niño being classified as EP events (dark red) in which $EPI > EP\ Thr$ and $CPI < CP\ Thr$. In this way, the 2015/16 and 1991/92 El Niños can be classified as both EP and CP (red), and the events in yellow are CP El Niños ($CPI > CP\ Thr$, $EPI < EP\ Thr$). The same applies for La Niñas but using negative thresholds. Note how the event classification can change with subtle shift in the thresholds. The size of the circles corresponds to the magnitude of the Niño3.4 anomaly: large circles for $|Ni\tilde{no}3.4| > 1.8\ sdev$; medium circles for $1\ sdev < |Ni\tilde{no}3.4| < 1.8\ sdev$; small circles for $0.5\ sdev < |Ni\tilde{no}3.4| < 1\ sdev$. Gray circles are considered as neutral years ($|Ni\tilde{no}3.4| < 0.5\ sdev$). The NOAA Extended Reconstructed SST version 5 (ERSSTv5; Huang et al. 2017) is used in this analysis with linear trends removed.

Figure 2. Surface air temperature (SAT) and rainfall anomaly patterns associated with (a) Eastern Pacific and (b) Central Pacific ENSO shown as the regression of SAT (color shading)

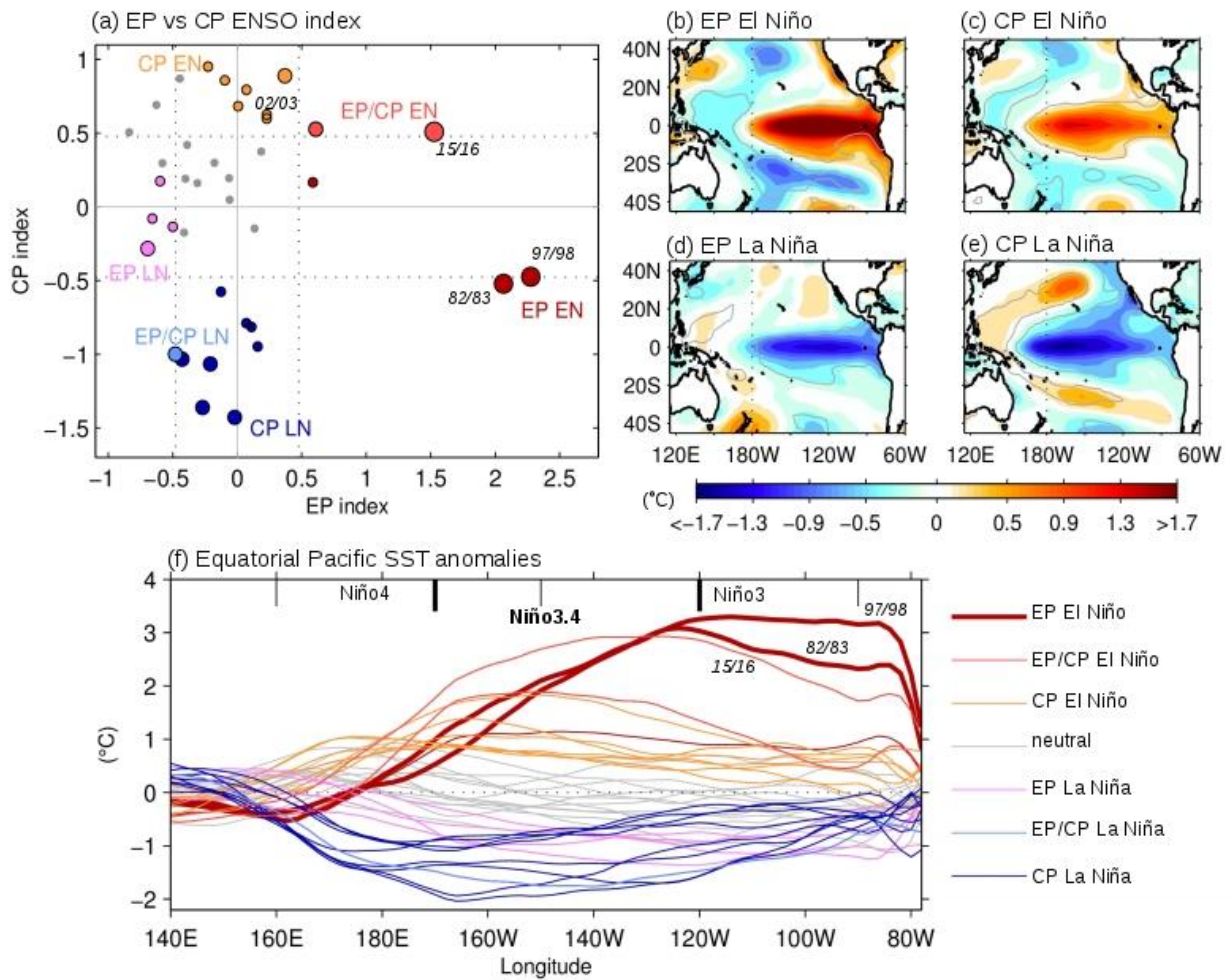
and rainfall anomalies (contours) against the EP and CP ENSO indices of Sullivan et al. (2016) defined in Fig. 1. Units are in $^{\circ}\text{C}$ and mm day^{-1} per standard deviation. The analysis uses monthly data of NCEP/NCAR Reanalysis (Kalnay et al. 1996) for SAT, CPC Merged Analysis of Precipitation (CMAP; Xie and Arkin 1997), and NOAA Extended Reconstructed SST version 5 (ERSSTv5; Huang et al. 2017) to calculate the ENSO indices from 1980 to 2016, with monthly climatology and long-term trends removed. Stippling indicates rainfall regression coefficients that are statistically significant above the 95% level.

Figure 3. ENSO Outlook of the Australian Bureau of Meteorology along with the anomaly of temperature averaged over the top 300 m in the equatorial Pacific Ocean as a proxy of warm water volume (WWV; black) and the Niño3.4 index (green) from January 2013 to February 2018. The outlook is produced based on a survey of Bureau’s own coupled seasonal forecast model and seven others from leading international climate agencies (generally WMO Global Producing Centers of Long Range Forecasts). The explanation for the outlook can be found in www.bom.gov.au/climate/enso/outlook/#tabs=ENSO-Outlook-history. The WWV data can be accessed from www.pmel.noaa.gov/tao/wwv/data/. The Niño3.4 index is an average of sea surface temperature (SST) over (5°S – 5°N , 170°W – 120°W) calculated based on NOAA ERSST version 5 (ERSSTv5) dataset (www.esrl.noaa.gov/psd/data/gridded/data.noaa.ersst.v5.html).

Figure 4. Climate model bias in sea surface temperature and ENSO seasonality as part of the many challenges facing ENSO research. (a) Difference in SST between multi-model ensemble mean and observed (ERSSTv5) exhibiting the classical ‘cold-tongue’ bias (color shading). The climatological observed and multi-model mean SSTs are shown in black and

red contours, respectively. Twenty CMIP5 models are utilized, with stippling indicating 18 or more models exhibiting the same sign in the bias. (b) Standard deviation of the Niño3.4 index in the CMIP5 models with annual mean of the standard deviation removed. Observed and multi-model mean seasonal climatologies are shown in thick black and red dashed lines, respectively, both indicate a peak of ENSO variability around austral summer and lowest variability in austral autumn. The most biased models in terms of the annual cycle are highlighted in thick colored lines.

Figure 5. Factors affecting ENSO and the societal implications. ENSO characteristics are influenced by many factors including coupled feedback processes, atmospheric and oceanic noise, and climate forcing from other oceanic basins, as well as the basic mean state which evolves on long time scales. All of these components interact with one another and are influenced by external forcing (e.g., greenhouse gasses, aerosols, solar variability), which in turn influences the predictability and impacts of ENSO.



978

979 **Figure 1.** ENSO diversity over 1980-2017. (a) Eastern Pacific (EP) ENSO index (EPI)
 980 versus Central Pacific (CP) index (CPI) averaged over December-February (DJF) when
 981 ENSO events typically peak, where circle size corresponds to ENSO amplitude and the color
 982 indicates the type (EP, CP, EP/CP). (b)-(e) Composite of DJF SST anomalies for each type
 983 of ENSO events. (f) SST anomaly over the equatorial Pacific (averaged over 5°S-5°N)
 984 marked by different colors that signify event types in (a). The EPI and CPI are based on
 985 those of Sullivan et al. (2016), defined as $\text{Niño3} - 0.5 \cdot \text{Niño4}$ and $\text{Niño4} - 0.5 \cdot \text{Niño3}$,
 986 respectively (where the Niño indices are first normalized). Niño3 and Niño4 indices are SST
 987 anomalies averaged over (5°S-5°N, 150°W-90°W) and (5°S-5°N, 160°E-150°W),
 988 respectively. An arbitrary threshold (Thr) can be applied to the indices to classify each year
 989 into EP, CP, or a mix (EP/CP). In this case, 0.7 of the index standard deviation (sdev.) is
 990 used (dotted lines), with the 1982/83 and 1997/98 extreme El Niño being classified as EP
 991 events (dark red) in which $\text{EPI} > \text{EP Thr}$ and $\text{CPI} < \text{CP Thr}$. In this way, the 2015/16 and

1991/92 El Niños can be classified as both EP and CP (red), and the events in yellow are CP El Niños ($CPI > CP\ Thr$, $EPI < EP\ Thr$). The same applies for La Niñas but using negative thresholds. Note how the event classification can change with subtle shift in the thresholds. The size of the circles corresponds to the magnitude of the Niño3.4 anomaly: large circles for $|Niño3.4| > 1.8\ sdev$; medium circles for $1\ sdev < |Niño3.4| < 1.8\ sdev$; small circles for $0.5\ sdev < |Niño3.4| < 1\ sdev$. Gray circles are considered as neutral years ($|Niño3.4| < 0.5\ sdev$). The NOAA Extended Reconstructed SST version 5 (ERSSTv5; Huang et al. 2017) is used in this analysis with linear trends removed.

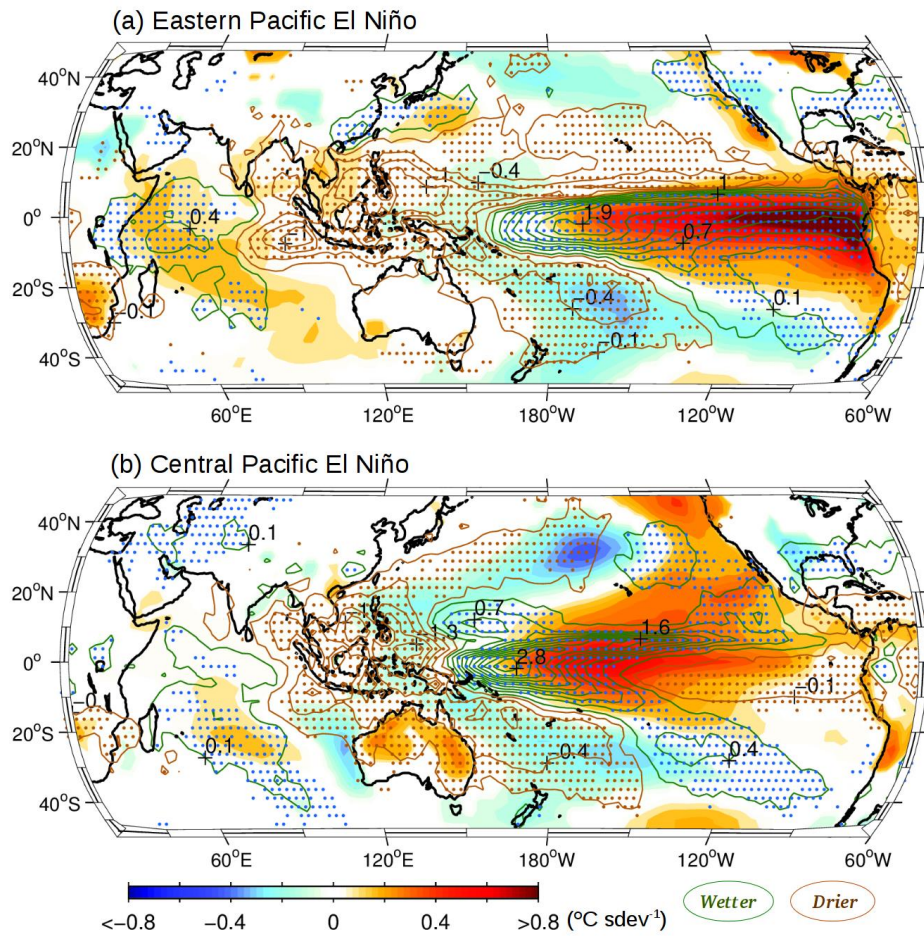


Figure 2. Surface air temperature (SAT) and rainfall anomaly patterns associated with (a) Eastern Pacific and (b) Central Pacific ENSO shown as the regression of SAT (color shading) and rainfall anomalies (contours) against the EP and CP ENSO indices of Sullivan et al. (2016). Units are in $^{\circ}\text{C}$ and mm day^{-1} per standard deviation. The analysis uses monthly data of NCEP/NCAR Reanalysis (Kalnay et al. 1996) for SAT, CPC Merged Analysis of Precipitation (CMAP; Xie and Arkin 1997), and NOAA Extended Reconstructed SST version 5 (ERSSTv5; Huang et al. 2017) to calculate the ENSO indices from 1980 to 2016, with monthly climatology and long-term trends removed. Stippling indicates rainfall regression coefficients that are statistically significant above the 95% level. The EP and CP ENSO indices are defined as $\text{Niño3} - 0.5 \cdot \text{Niño4}$ and $\text{Niño4} - 0.5 \cdot \text{Niño3}$, respectively (where the Niño indices are first normalized). Niño3 and Niño4 indices are SST anomalies averaged over $(5^{\circ}\text{S} - 5^{\circ}\text{N}, 150^{\circ}\text{W} - 90^{\circ}\text{W})$ and $(5^{\circ}\text{S} - 5^{\circ}\text{N}, 160^{\circ}\text{E} - 150^{\circ}\text{W})$, respectively.

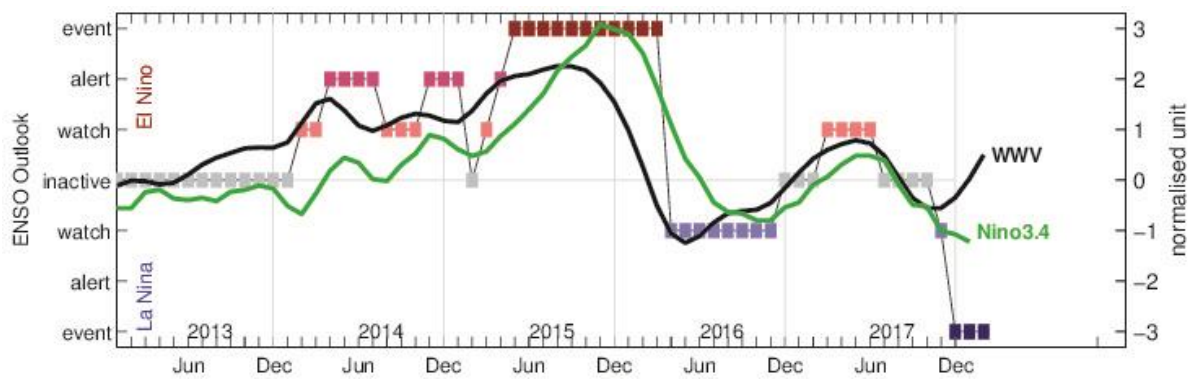


Figure 3. ENSO Outlook of the Australian Bureau of Meteorology along with the anomaly of temperature averaged over the top 300 m in the equatorial Pacific Ocean as a proxy of warm water volume (WWV; black) and the Niño3.4 index (green) from January 2013 to February 2018. The outlook is produced based on a survey of Bureau's own coupled seasonal forecast model and seven others from leading international climate agencies (generally WMO Global Producing Centers of Long Range Forecasts). The explanation for the outlook can be found in www.bom.gov.au/climate/enso/outlook/#tabs=ENSO-Outlook-history. The WWV data can be accessed from www.pmel.noaa.gov/tao/wwv/data/. The Niño3.4 index is an average of sea surface temperature (SST) over (5°S–5°N, 170°W–120°W) calculated based on NOAA ERSST version 5 (ERSSTv5) dataset (www.esrl.noaa.gov/psd/data/gridded/data.noaa.ersst.v5.html).

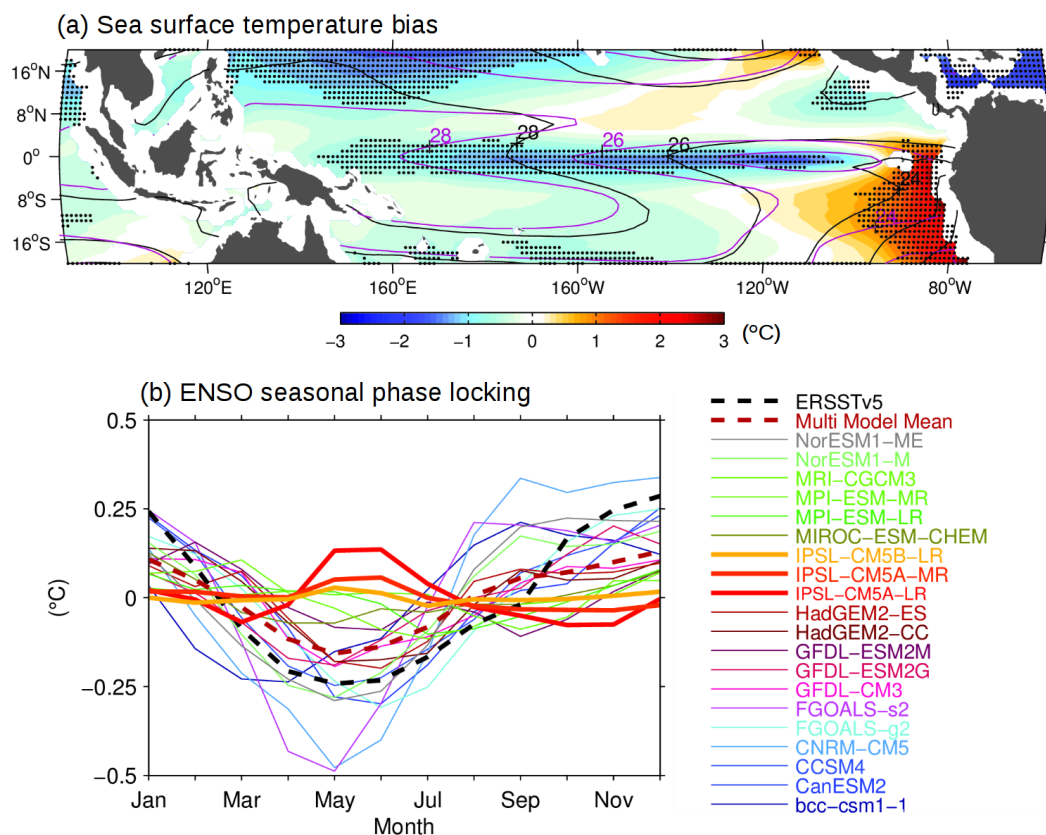


Figure 4. Climate model bias in sea surface temperature and ENSO seasonality as part of the many challenges facing ENSO research. (a) Difference in SST between multi-model ensemble mean and observed (ERSSTv5) exhibiting the classical ‘cold-tongue’ bias (color shading). The climatological observed and multi-model mean SSTs are shown in black and red contours, respectively. Twenty CMIP5 models are utilized, with stippling indicating 18 or more models exhibiting the same sign in the bias. (b) Standard deviation of the Niño3.4 index in the CMIP5 models with annual mean of the standard deviation removed. Observed and multi-model mean seasonal climatologies are shown in thick black and red dashed lines, respectively, both indicate a peak of ENSO variability around austral summer and lowest variability in austral autumn. The most biased models in terms of the annual cycle are highlighted in thick colored lines.

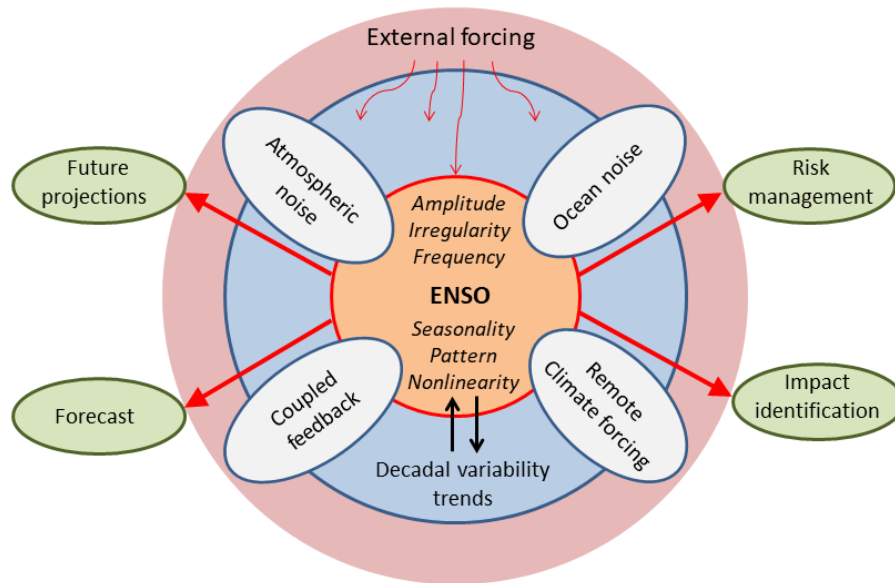


Figure 5. Factors affecting ENSO and the societal implications. ENSO characteristics are influenced by many factors including coupled feedback processes, atmospheric and oceanic noise, and climate forcing from other oceanic basins, as well as the basic mean state which evolves on long time scales. All of these components interact with one another and are influenced by external forcing (e.g., greenhouse gasses, aerosols, solar variability), which in turn influences the predictability and impacts of ENSO.